

Supporting Information

Co-crystal $\text{LiCl} \cdot (\text{H}_3\text{C}_3\text{N}_3\text{O}_3)$: A Promising Solar-blind Nonlinear Optical Crystals with Giant Nonlinearity from Coplanar π -conjugated Groups

Fei Liang, Naizheng Wang, Xiaomeng Liu, Zheshuai Lin,* and Yicheng Wu

Contents

1. **Computational methods**
2. **Figure S1.** The molecular orbitals of $(\text{COOH})^-$ and $(\text{NO}_2)^-$ groups.
3. **Figure S2.** The electronic localized function (ELF) map of $(\text{C}_3\text{N}_3\text{O}_3)^{3-}$, $(\text{HC}_3\text{N}_3\text{O}_3)^{2-}$, $(\text{H}_2\text{C}_3\text{N}_3\text{O}_3)^-$ and $\text{H}_3\text{C}_3\text{N}_3\text{O}_3$
4. **Figure S3.** The electron density map of LCHCY crossing the ab plane
5. **Figure S4.** The band structures of LCHCY calculated by (a) PEBsol and (b) HSE06 functional.
6. **Figure S5.** The refractive index dispersion of LCHCY ranged from 250 to 1200 nm.
7. **Figure S6.** The band structures of LCCY calculated by PEBsol functional.
8. **References**

Computational methods

The first-principles calculations are performed by the pseudopotential¹ methods implemented in the CASTEP package² based on the density functional theory (DFT).³ The optimized norm-conserving pseudopotentials⁴ are used to simulate ion-electron interactions for all constituent elements. A kinetic energy cutoff of 800 eV is chosen with Monkhorst-Pack k-point meshes spanning less than $0.04/\text{\AA}^3$ in the Brillouin zone.⁵ The cell parameters and the atomic positions in the unit cells of all crystals are fully fixed during optical properties calculations. Based on the calculated electronic structure, the imaginary part of the dielectric function is calculated and the real part of the dielectric function is determined using the Kramers–Kronig transform,⁶ and then the refractive indices n and the birefringence Δn are obtained. The shortest SHG output wavelength λ_{PM} is calculated based on the dispersion curves of refractive index (e.g., n_o and n_e), satisfying the condition of $n_o(2\lambda_{\text{PM}}) = n_e(\lambda_{\text{PM}})$.

The second order susceptibility $\chi^{(2)}$ and SHG coefficient d_{ij} ($d_{ij} = 1/2 \chi^{(2)}$) is calculated using an expression originally proposed by Rashkeev *et al*⁷ and developed by Lin *et al*:⁸

$$\chi_{ijk} = \chi_{ijk}(\text{VE}) + \chi_{ijk}(\text{VH}) + \chi_{ijk}(\text{twobands}) \quad (1)$$

where χ_{ijk} (VE), χ_{ijk} (VH) and χ_{ijk} (two bands) denote the contributions from virtual-electron processes, virtual-hole processes and two band processes, respectively. In detail, the formulae for calculating χ_{ijk} (VE), χ_{ijk} (VH) and χ_{ijk} (two bands) are as follows:

$$\chi_{ijk}(\text{VE}) = \frac{e^3}{2\hbar^2 m^3} \sum_{vcc'} \int \frac{d^3 k}{4\pi^3} P(ijk) \text{Im}[p_{vc}^i p_{cc'}^j p_{c'v}^k] \left(\frac{1}{\omega_{cv}^3 \omega_{v'c'}^2} + \frac{2}{\omega_{vc}^4 \omega_{c'v}} \right), \quad (2)$$

$$\chi_{ijk}(\text{VH}) = \frac{e^3}{2\hbar^2 m^3} \sum_{vv'c} \int \frac{d^3 k}{4\pi^3} P(ijk) \text{Im}[p_{vv'}^i p_{v'c}^j p_{cv}^k] \left(\frac{1}{\omega_{cv}^3 \omega_{v'c}^2} + \frac{2}{\omega_{vc}^4 \omega_{cv'}} \right), \quad (3)$$

$$\chi_{ijk}(\text{twobands}) = \frac{e^3}{\hbar^2 m^3} \sum_{vc} \int \frac{d^3 k}{4\pi^3} P(ijk) \frac{\text{Im}[p_{vc}^i p_{cv}^j (p_{vv}^k - p_{cc}^k)]}{\omega_{vc}^5} \quad (4)$$

Here, i, j and k are Cartesian components; v and v' denote VB, and c and c' denote CB. $P(ijk)$ denotes full permutation. It is noted that the refractive indices and SHG coefficients can be accurately obtained by DFT in principle because these optical properties are determined by the virtual electronic excited processes, which are described by the first and second order perturbations on the ground state wave functions, respectively.

Furthermore, it should be emphasized that the generalized gradient approximation (GGA) method with PBEsol functional⁹ usually heavily underestimates the energy bandgap E_g , while the hybrid HSE06 method can make an accurate prediction for metal cyanurates.^{10–12} Herein, the scissors-corrected¹³ GGA method is employed to calculate the optical properties, where the scissors operator is set as the difference between the HSE06 and GGA bandgaps. This self-consistent *ab initio* approach has been proven to be an efficient way for the investigation of linear and NLO properties in many types of NLO materials without introducing any experimental parameter.^{14–15}

The cohesive energy E_{coh} was defined as,

$$E_{\text{coh}} = E_{(\text{crystal})} - N_1 E_{(\text{anionic group})} - N_2 E_{(\text{Li}^+)} - N_3 E_{(\text{Cl}^-)}$$

Where E_{crystal} is the total energy of LCHCY and LCCY crystal; $E_{(\text{anionic group})}$ is the total of cyanuric acid molecule and electronegative $(\text{C}_3\text{N}_3\text{O}_3)^{3-}$ group; $E_{(\text{Li}^+)}$ and $E_{(\text{Cl}^-)}$ are the energy of lithium and chlorine

ions; the N_1 , N_2 and N_3 are the number of anionic group, lithium and chlorine ions. According to the above definitions, a negative E_{coh} value corresponds to an exothermic reaction, and the more negative the E_{coh} means the more stable compound.

Figure S1. The molecular orbitals of $(\text{COOH})^-$, $(\text{NO}_2)^-$ and $(\text{HC}_3\text{N}_3\text{O}_3)^{2-}$ groups

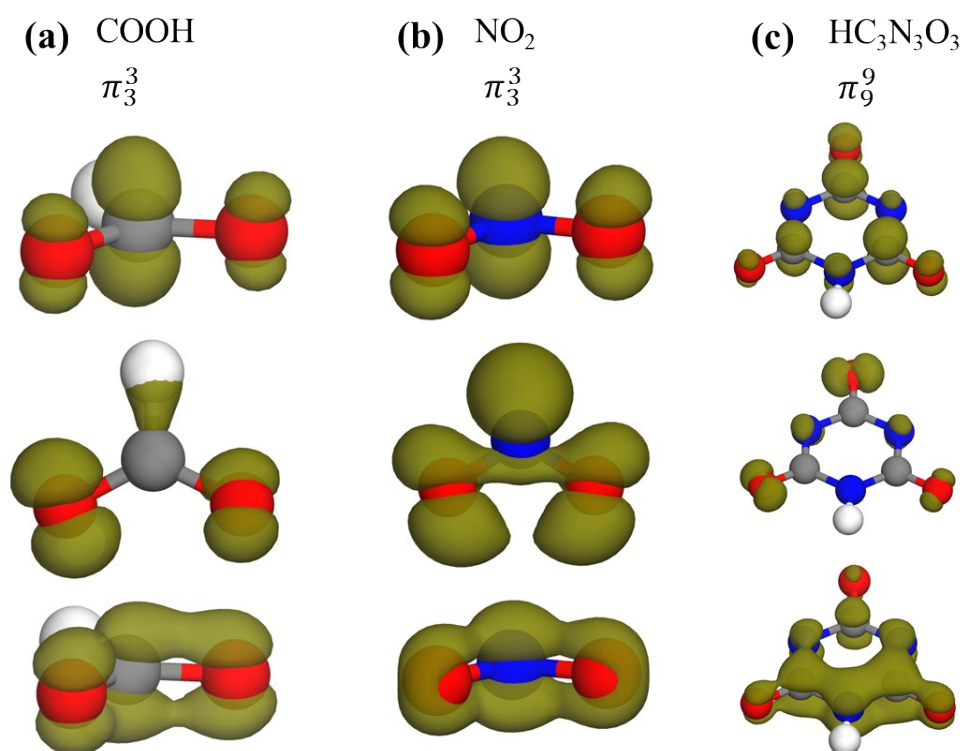


Figure S2. The electronic localized function (ELF) map of $(\text{C}_3\text{N}_3\text{O}_3)^{3-}$, $(\text{HC}_3\text{N}_3\text{O}_3)^{2-}$, $(\text{H}_2\text{C}_3\text{N}_3\text{O}_3)^{-}$ and $\text{H}_3\text{C}_3\text{N}_3\text{O}_3$

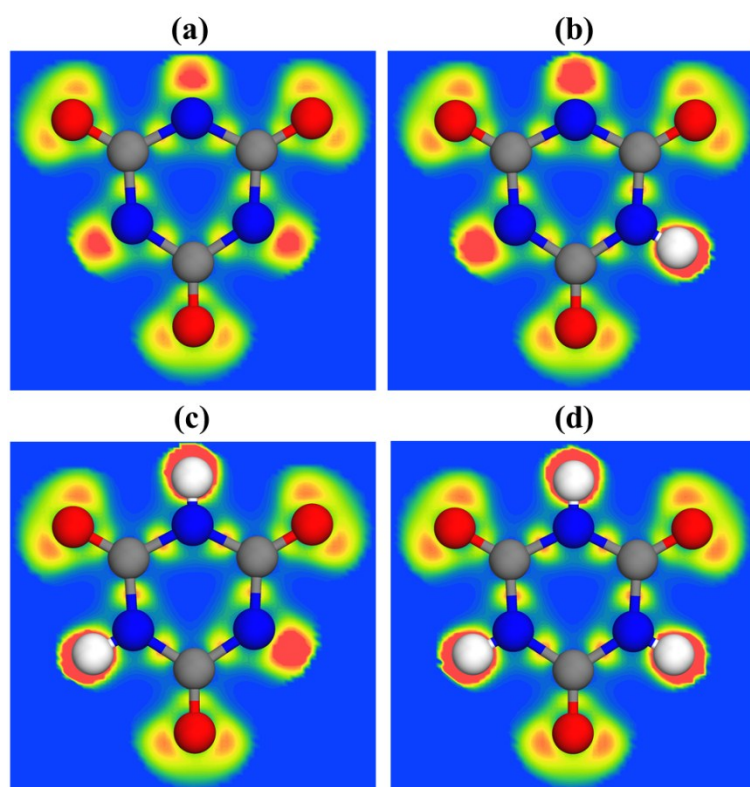


Figure S3. The electron density map of LCHCY crossing the ab plane, The gray, blue, red, white and green balls represent the C, N, O, H, and Cl atoms, respectively.

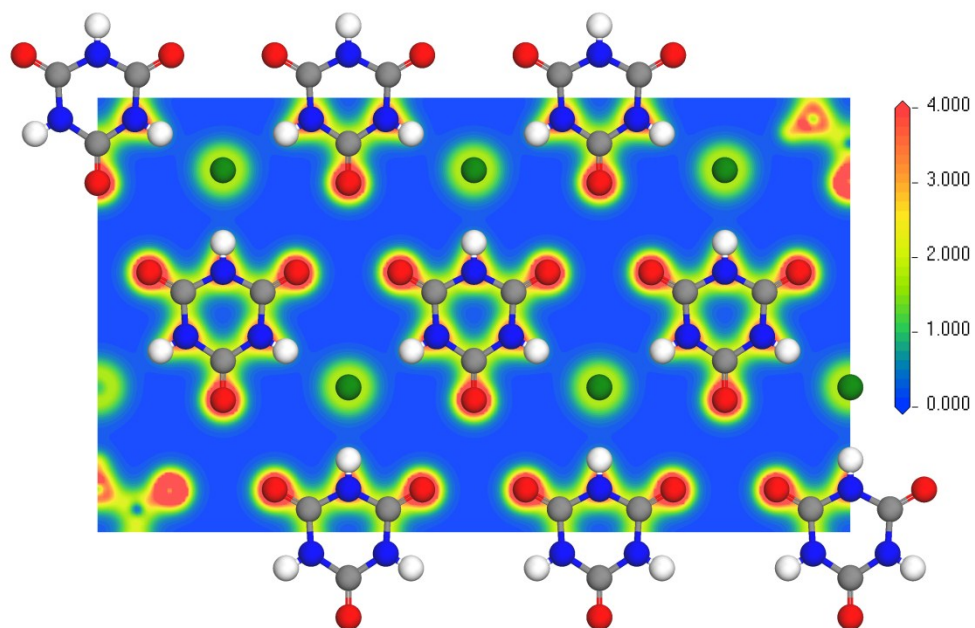


Figure S4. The band structures of LCHCY calculated by (a) PEBsol and (b) HSE06 functional.

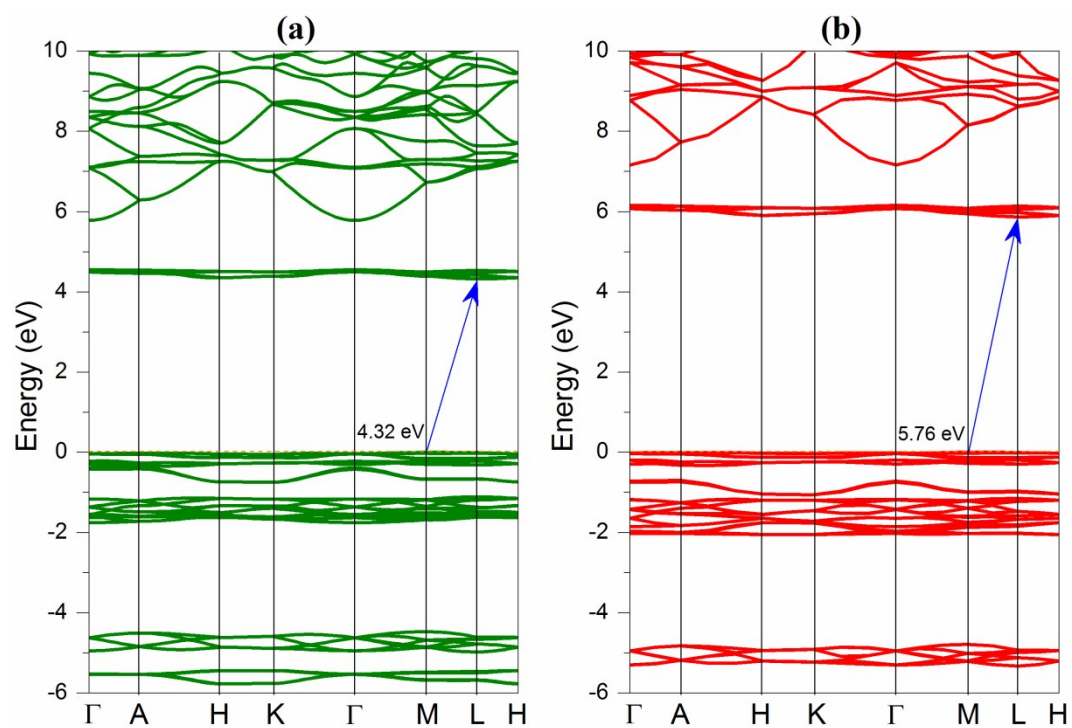


Figure S5. The refractive index dispersion of LCHCY ranged from 250 to 1200 nm.

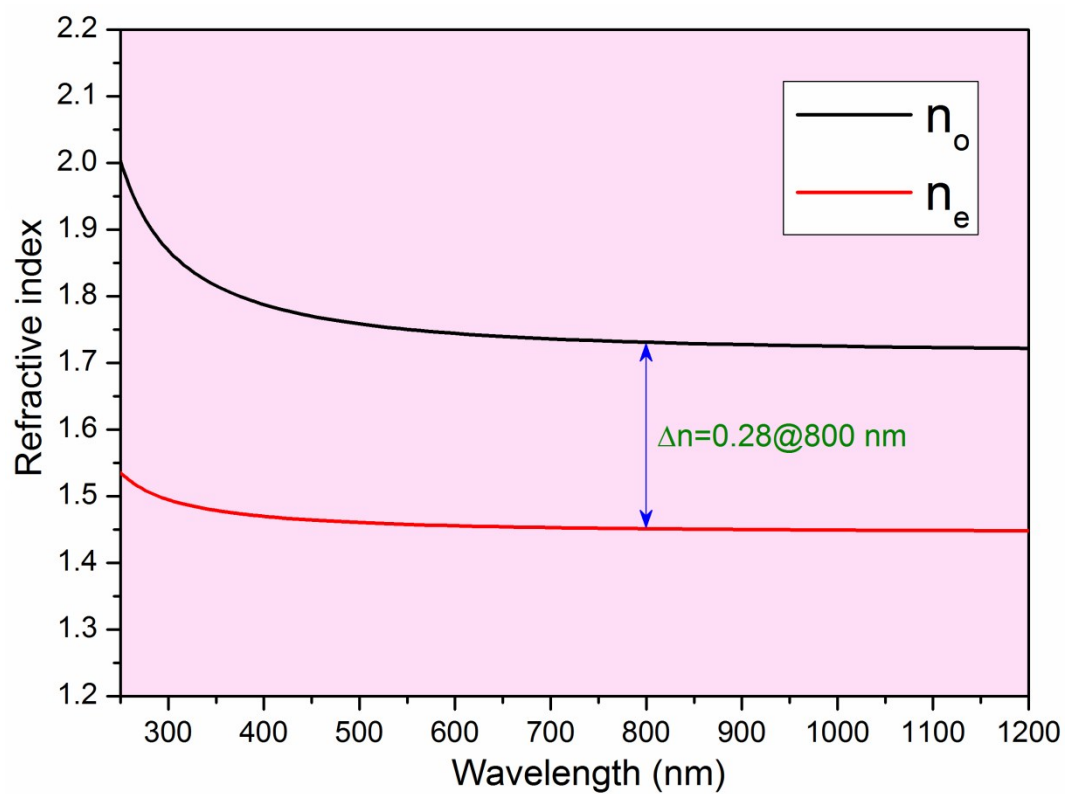
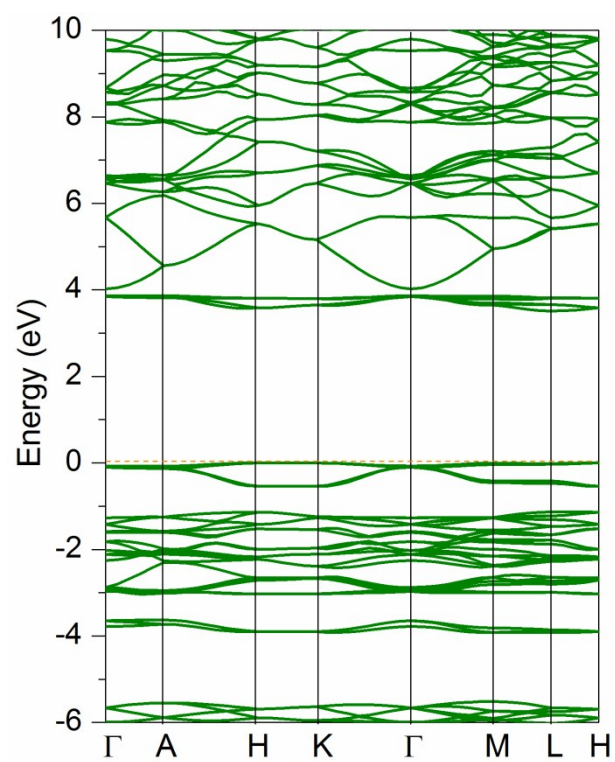


Figure S6. The band structures of LCCY calculated by PEBsol functional.



References

- (1) Payne, M. C.; Teter, M. P.; Allan, D. C.; Arias, T. A.; Joannopoulos, J. D., *Rev. Mod. Phys.* **1992**, *64*, 1045-1097.
- (2) Clark, S. J.; Segall, M. D.; Pickard, C. J.; Hasnip, P. J.; Probert, M. J.; Refson, K.; Payne, M. C., *Z. Kristallogr.* **2005**, *220*, 567-570.
- (3) Kohn, W., *Rev. Mod. Phys.* **1999**, *71*, 1253-1266.
- (4) Rappe, A. M.; Rabe, K. M.; Kaxiras, E.; Joannopoulos, J. D., *Phys. Rev. B* **1990**, *41*, 1227-1230.
- (5) Monkhorst, H. J.; Pack, J. D., *Phys. Rev. B* **1976**, *13*, 5188-5192.
- (6) Kang, L.; Ramo, D. M.; Lin, Z.; Bristowe, P. D.; Qin, J.; Chen, C., *J. Mater. Chem. C* **2013**, *1*, 7363-7370.
- (7) Rashkeev, S. N.; Lambrecht, W. R. L.; Segall, B., *Phys. Rev. B* **1998**, *57*, 3905-3919.
- (8) Lin, J.; Lee, M. H.; Liu, Z. P.; Chen, C. T.; Pickard, C. J., *Phys. Rev. B* **1999**, *60*, 13380-13389.
- (9) Perdew, J. P.; Burke, K.; Ernzerhof, M., *Phys. Rev. Lett.* **1996**, *77*, 3865-3868.
- (10) Xia, M.; Zhou, M.; Liang, F.; Meng, X.; Yao, J.; Lin, Z.; Li, R., *Inorg. Chem.* **2018**, *57*, 32-36.
- (11) Li, Z.; Liang, F.; Guo, Y.; Lin, Z.; Yao, J.; Zhang, G.; Yin, W.; Wu, Y.; Chen, C., *J. Mater. Chem. C* **2018**, *6*, 12879-12887.
- (12) Tang, J.; Liang, F.; Meng, X.; Kang, K.; Yin, W.; Zeng, T.; Xia, M.; Lin, Z.; Yao, J.; Zhang, G.; Kang, B., *Cryst. Growth & Des.* **2019**, *19*, 568-572.
- (13) Wang, C. S.; Klein, B. M., *Phys. Rev. B* **1981**, *24*, 3417-3429.
- (14) Lin, Z. S.; Jiang, X. X.; Kang, L.; Gong, P. F.; Luo, S. Y.; Lee, M. H., *Journal of Physics D-Applied Physics* **2014**, *47*, 253001.
- (15) Liang, F.; Kang, L.; Zhang, X.; Lee, M.; Lin, Z.; Wu, Y., *Cryst. Growth & Des.* **2017**, *17*, 4015-4020.